ENHANCED KNOWLEDGE IN SCIENCES AND TECHNOLOGY
e-ISSN: 2773-6385

EKST

Vol. 4 No. 2 (2024) 8-15
https://publisher.uthm.edu.my/periodicals/index.php/ekst

Solving Blasius Hybrid Nanofluid Flow Over a Permeable Plate Using the Shooting Technique

Mohammad Arief Haiqal Radzuan[1], Fazlina Aman[2]*

[1] *Department of Mathematics and Statistics, Faculty of Applied Sciences and Technology, UTHM Kampus Cawangan Pagoh, Hab Pendidikan Tinggi Pagoh, KM1, Jalan Panchor, 84600 Pagoh, Muar, Johor, MALAYSIA*

*Corresponding Author: fazlina@uthm.edu.my
DOI: https://doi.org/10.30880/ekst.2024.04.02.002

Article Info

Received: 27 December 2023
Accepted: 11 January 2024
Available online: 12 December 2024

Keywords

Blasius Flow, Hybrid Nanofluid, Heat Transfer, Permeable Plate, Shooting Technique

Abstract

The study uses a shooting technique to examine the laminar boundary layer flow of a Blasius flow with Cu-Al_2O_3 hybrid nanoparticles over a permeable plate. Using similarity transformation to transform the model from partial differential equations to ordinary differential equations using the governing equation, the study takes into consideration the effects of radiation and viscous dissipation. The solutions are then obtained by using the shooting technique with the RKF45 method in Maple software. Hybrid nanoparticles demonstrate advantageous thermal properties resulting from synergistic effects, although these effects wane with a rise in the Eckert number. These findings help improve productivity and plan processes for specific products according to desired output. This important early study offers valuable insights for engineers and scientists, guiding future applications.

1. Introduction

Due to the enhanced thermophysical characteristics, nanofluids colloidal suspensions of nanoparticles in a base fluid have attracted a lot of attention. Hybrid nanofluids consist of blends of two or more distinct types of nanoparticles distributed in a base fluid. These nanofluids have demonstrated improved heat transfer characteristics compared to traditional fluids, positioning them as promising candidates for various engineering applications.

The smooth, steady flow of a viscous fluid across a flat plate is known as "Blasius flow". The Blasius solution, which has been extensively researched in fluid dynamics and heat transfer, presents an analytical solution for the velocity and temperature profiles in such a flow given by [1].

Research in recent years has focused on the exploration of fluid flow and heat transfer characteristics over permeable plates. Research conducted by [2], the focus of the study was to comprehend the behaviour of hybrid nanofluids over a non-linear permeable stretching/shrinking surface. Permeable plates, which enable fluid flow through their porous structure, are integral to various engineering applications, including filtration, separation, and heat exchange.

The study aimed to analyse the interactions between the hybrid nanofluid and the permeable plate while examining the resulting flow and heat transfer characteristics. This research contributes valuable insights into the understanding of fluid dynamics and heat transfer phenomena specifically related to permeable plates, providing useful knowledge for practical engineering applications. The Blasius hybrid nanofluid flow over a permeable plate is hence the focus of this study. The objective is to comprehend the mathematical formulation and attempt to use the shooting method to solve the issue.

2. Mathematical Formulation

According to the depicted physical model in Figure 1, there is a uniform upstream velocity U_∞ along the *x*-axis. Furthermore, $u = U_w$ is utilized to denote the constant velocity of the plate. The flow is also influenced by the radiative heat flux q_r, which acts in the positive y-direction perpendicular to the surface. The impact of viscous dissipation has been factored in. Additionally, the study assumes the consideration of a stable hybrid nanofluid, implying that there is no consideration for nanoparticle sedimentation/aggregation. The spherical shape and homogeneous size of the nanoparticles are among the presumed properties. Additionally, it is assumed that the base fluid and the nanoparticles are flowing at the same velocity in a state of thermal equilibrium by referring to [3]

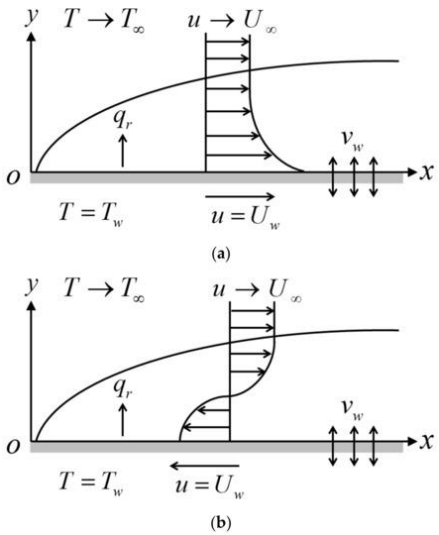

Fig. 1 The fluid and plate flow configurations can either move in the assisting flows (a) or in the opposing flows (b) ([3])

In accordance with [4], [1], and [5], the governing equations for the hybrid nanofluid are as follows:

$$\frac{\partial u}{\partial x} + \frac{\partial v}{\partial y} = 0 \tag{1}$$

$$u\frac{\partial u}{\partial x} + v\frac{\partial u}{\partial y} = \frac{\mu_{hnf}}{\rho_{hnf}}\frac{\partial^2 u}{\partial y^2}, \tag{2}$$

$$u\frac{\partial T}{\partial x} + v\frac{\partial T}{\partial y} = \frac{k_{hnf}}{\left(\rho C_p\right)_{hnf}}\frac{\partial^2 T}{\partial y^2} + \frac{\mu_{hnf}}{\left(\rho C_p\right)_{hnf}}\left(\frac{\partial u}{\partial y}\right)^2 - \frac{1}{\left(\rho C_p\right)_{hnf}}\frac{\partial q_r}{\partial y} \tag{3}$$

Under the given boundary conditions, these can be written as follows:

$$u = U_w,\ v = v_w(x),\ T = T_w \ at\ y = 0,$$
$$u \to U_\infty,\ T \to T_\infty \ as\ y \to \infty \tag{4}$$

where (u, v) denotes the mass flow velocity $v_w(x)$ and represents the velocities in the (x, y) axes, respectively. Furthermore, the temperature is indicated by T, along with constant wall and free stream temperatures, indicated by T_∞ and T_w, respectively. Concerning [6], the radiative heat flux expression is as follows:

Enhanced Knowledge in Sciences and Technology Vol. 4 No. 2 (2024) p. 8-15

$$q_r = -\frac{4\sigma^*}{3k^*}\frac{\partial T^4}{\partial y}, \tag{5}$$

where σ^* and k^* are the Stefan-Boltzmann constant and Rosseland mean absorption coefficient, respectively. Following Rosseland *et al.* (1931), $T^4 \cong 4T^3{}_\infty T - 3T^4$ which transform (3) to:

$$u\frac{\partial T}{\partial x} + v\frac{\partial T}{\partial y} = \frac{1}{(\rho C_p)_{hnf}}\left[k_{hnf} + \frac{16\sigma^* T^3{}_\infty}{3k^*}\right]\frac{\partial^2 T}{\partial y^2} + \frac{\mu_{hnf}}{(\rho C_p)_{hnf}}\left(\frac{\partial u}{\partial y}\right)^2 \tag{6}$$

Using the formulas from the previous work, we determined the hybrid nanofluid's thermophysical characteristics, which are listed in Table 1. The volume fractions of Al_2O_3 and Cu nanoparticles are indicated as φ_1 and φ_2, respectively, in this context. In the meantime, the values for dynamic viscosity, density, heat capacity, specific heat at constant pressure, and thermal conductivity are $\mu, \rho, C_p, (\rho C_p)$ and k respectively. Properties pertaining to Al_2O_3, Cu, hybrid nanofluid, nanofluid, and fluid are indicated by the subscripts η_1, η_2, hnf, nf and f respectively. Table 2 lists the physical characteristics of the base fluid and the nanoparticles.

Table 1 Thermophysical properties of nanofluid and hybrid nanofluid ([7])

Thermophysical Properties	Correlations
Thermal conductivity	$\frac{k_{hnf}}{k_f} = \frac{\frac{\varphi_1 k_{\eta 1} + \varphi_2 k_{\eta 2}}{\varphi_{hnf}} + 2k_f - 2(\varphi_1 k_{\eta 1} + \varphi_2 k_{\eta 2}) - 2\varphi_{hnf} k_f}{\frac{\varphi_1 k_{\eta 1} + \varphi_2 k_{\eta 2}}{\varphi_{hnf}} + 2k_f - (\varphi_1 k_{\eta 1} + \varphi_2 k_{\eta 2}) + \varphi_{hnf} k_f}$
Heat capacity	$(\rho C_p)_{hnf} = (1-\varphi_{hnf})(\rho C_p)_f + \varphi_1 (\rho C_p)_{n1} + \varphi_2 (\rho C_p)_{n2}$
Density	$\rho_{hnf} = (1-\varphi_{hnf})\rho_f + \varphi_1 \rho_{n1} + \varphi_2 \rho_{n2}$
Dynamic viscosity	$\mu_{hnf} = \frac{\mu_f}{(1-\varphi_{hnf})^{2.5}}$

Table 2 Thermophysical properties of the fluid and nanoparticles ([8])

Properties	Base Fluid	Nanoparticles	
	Water	Cu	Al2O3
$\rho(kg/m^3)$	997.1	8933	3970
$C_p(J/kgK)$	4179	385	765
$k(W/mK)$	0.613	400	40
Prandtl number,Pr	6.2		

2.1 Similarity transformation

By referring to [4] and [1], the similarity variables are as follows:

$$\psi = \sqrt{U_\infty \nu_f x}\, f(\eta),\ \theta(\eta) = \frac{T - T_\infty}{T_w - T_\infty},\ \eta = y\sqrt{\frac{U_\infty}{\nu_f x}}, \tag{7}$$

where $u = \partial\psi/\partial y$ and $v = -\partial\psi/\partial x$ such that

$$u = U_\infty f'(\eta),\quad v = -\frac{1}{2}\sqrt{\frac{U_\infty \nu_f}{x}}\left[f(\eta) - \eta f'(\eta)\right] \tag{8}$$

From (8), by setting $\eta = 0$, we obtain :

$$v_w(x) = -\frac{1}{2}\sqrt{\frac{U_\infty \nu_f}{x}}S \tag{9}$$

ν_f indicates the kinematic viscosity of the underlying fluid in this case. Additionally, the suction/injection parameter $f(0) = S$ where $S<0$ (injection) and $S>0$ (suction) denote permeable cases and $S=0$ represents an impermeable case determines the surface's permeability. Equation (1) is also satisfied when Equations (7) and (8) are used. Equations (2) and (6) are therefore reduced to:

$$\frac{\mu_{hnf}/\mu_f}{\rho_{hnf}/\rho_f} f''' + \frac{1}{2} f f'' = 0. \tag{10}$$

$$\frac{1}{Pr}\,\frac{1}{(\rho C_p)_{hnf}/(\rho C_p)_f}\left(\frac{k_{hnf}}{k_f} + \frac{4}{3}R\right)\theta'' + \frac{1}{2} f\theta' + Ec\left(\frac{\mu_{hnf}/\mu_f}{(\rho C_p)_{hnf}/(\rho C_p)_f}\right) f''^2 = 0. \tag{11}$$

with the boundary conditions:

$$\begin{aligned} &f(0) = S, f'(0) = \lambda, \theta(0) = 1 \\ &f'(\eta) \to 1, \theta(\eta) \to 0\ as\ \eta \to \infty \end{aligned} \tag{12}$$

The local skin friction coefficient and local Nusselt number, which are defined as follows, are the physical quantities of interest:

$$C_f = \frac{\mu_{hnf}}{\rho_f U_\infty^2}\left(\frac{\partial u}{\partial y}\right)_{y=0},$$

$$Nu_x = \frac{x}{k_f\left(T_w - T_\infty\right)}\left(-k_{hnf}\left(\frac{\partial T}{\partial y}\right)_{y=o} + \left(q_r\right)_{y=0}\right) \tag{13}$$

Using equations Eq. (7) and Eq. (13) we obtain:

$$Re_x^{1/2} C_f = \frac{\mu_{hnf}}{\mu_f} f''(0),\ Re_x^{1/2} Nu_x = -\left(\frac{k_{hnf}}{k_f} + \frac{4}{3}R\right)\theta'(0) \tag{14}$$

Enhanced Knowledge in Sciences and Technology Vol. 4 No. 2 (2024) p. 8-15

where the local Reynold number is given as $Re_x = U_\infty x / v_f$.

3. Results and Discussion

Using Maple's shooting method and Runge-Kutta-Fehlberg (RFK45), the similarity equations (9) and (10) are solved numerically, subject to the boundary condition equation (11). Tables and graphs are used to illustrate the outcomes analysis. In this investigation, the base fluid receives additions of 0.01 solid volume fractions of Cu and 0.01 solid volume of Al_2O_3. As a result, different solid volume fractions of copper are added to produce a hybrid nanofluid of Cu- Al_2O_3/water. The majority of the results of the research are produced using the base fluid's Prandtl number, which remains at $\Pr = 6.2$. Utilising Maple, the local Nusselt number $\theta'(0)$ and the skin friction coefficient $f''(0)$ are successfully determined. The Prandtl number $\Pr$, nanoparticle volume fraction for copper φ_2 ,nanoparticle volume fraction for alumina φ_1, radiation parameter, R and transpiration parameter ,S values are all the same as they were in the previous research.

Table 3 The result values of $f''(0)$ for variant of φ_1 when $\varphi_2 = \lambda = R = Ec = 0$

φ_1	[4]	[3]	Present results
0	0.3321	0.33206	0.33206
0.002	0.3339	0.33388	0.33388
0.004	0.3357	0.33571	0.33571
0.008	0.3394	0.33938	0.33938
0.01	0.3412	0.34123	0.34123

Table 4 The result values of $-\theta'(0)$ for variant of φ_1 when $\varphi_2 = \lambda = R = Ec = 0$

φ_1	Khasi'ie *et al.* [3]	Present results
0	0.62007	0.62007
0.002	0.62241	0.62241
0.004	0.62475	0.62475
0.008	0.62943	0.62943
0.01	0.63177	0.63177

In Table 3, it is observed that the skin friction coefficient increases with a rise of φ_1 from 0 to 0.01. As φ_1 increases, there is a corresponding augmentation in skin friction. The introduction of additional nanoparticles into the flow results in reduced flow motion, concurrently thinning the momentum boundary layer. Furthermore, the variation of the local Nusselt number, $\theta'(0)$, for different values of φ_1 is systematically explored under the conditions of $\varphi_2 = \lambda = R = Ec = 0$,and $\Pr = 6.2$ as delineated in Table 4. This table is included for future reference, providing a comprehensive overview of the heat transfer characteristics under varied nanoparticle concentrations. A noteworthy observation emerges from Table 3.2 where in the present of φ_1, the rate of heat transfer at the surface experiences an increase. It can also be seen from both Table 3 and Table 4 that the comparison results are in good agreement.

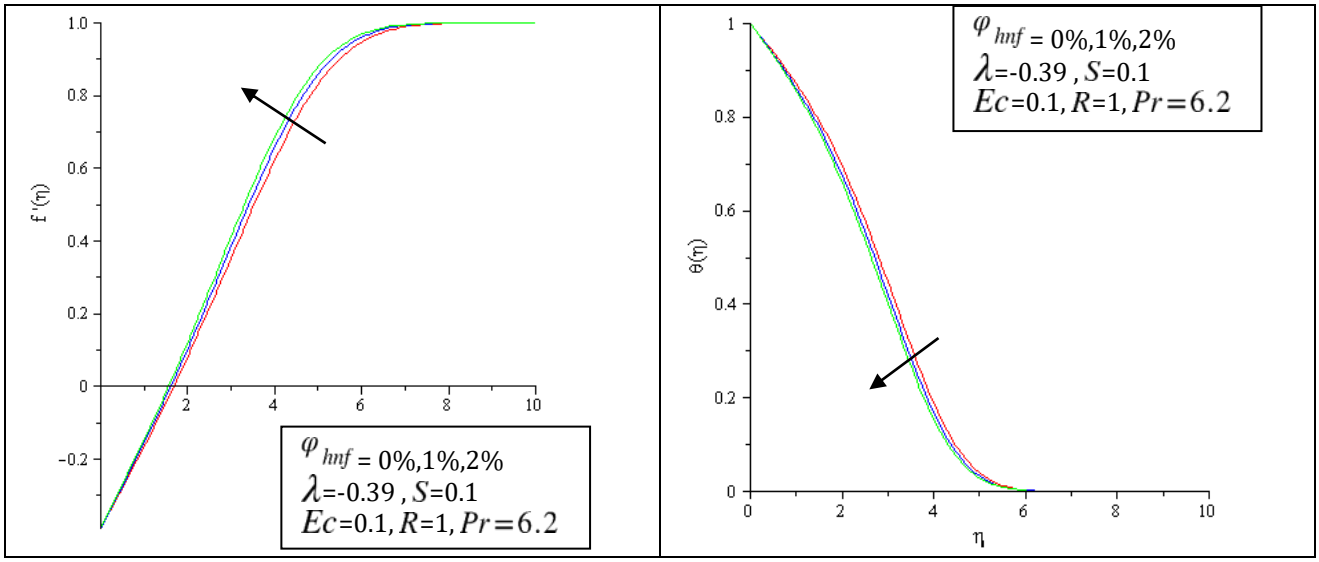

Fig. 2 Velocity profile, $f'(\eta)$ and temperature profile, $\theta(\eta)$ for various values of φ_{hnf}.

In Fig. 2, the increase in φ_{hnf} contributes to the increase of $f'(\eta)$. It can be observed that as the temperature profiles $\theta(\eta)$ decrease the nanoparticle volume fractions of Al_2O_3 increases. Therefore, the effect of nanoparticle volume fractions of Al_2O_3 is to decrease the heat transfer rate at the surface of the hybrid nanofluid. Besides, the effect of nanoparticle volume fractions of Al_2O_3 is to increase the velocity profiles of the hybrid nanofluid.

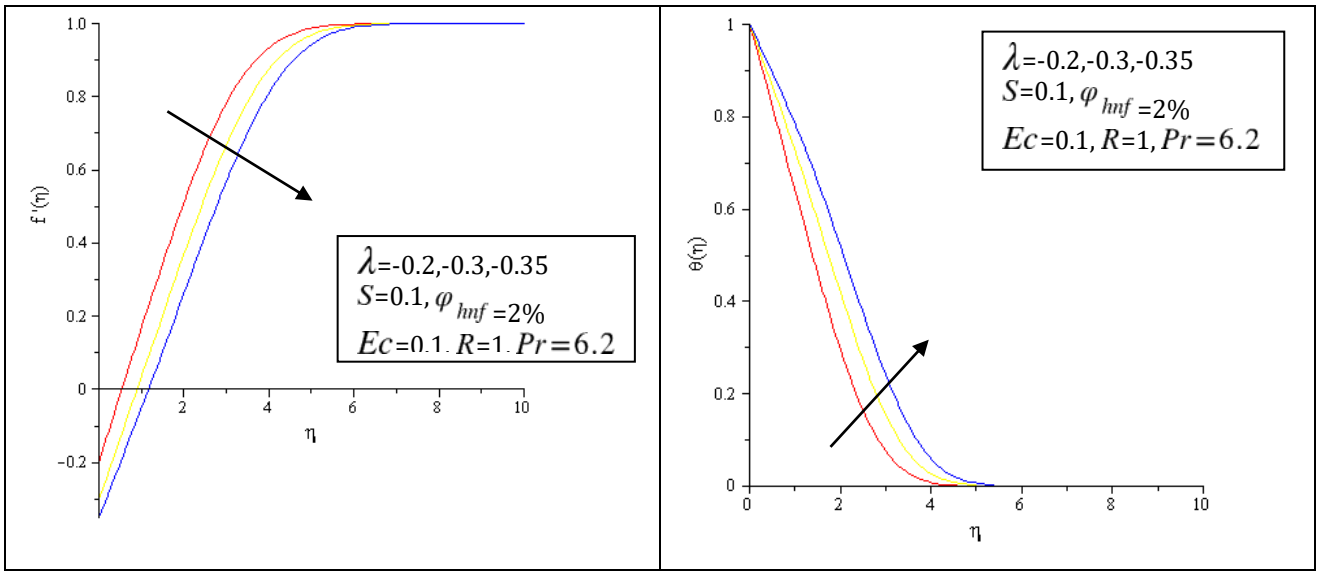

Fig. 3 Velocity profile, $f'(\eta)$ and temperature profile, $\theta(\eta)$ for various values of λ

Moreover, Fig. 3 illustrate the consequence of $\lambda<0$ on $f'(\eta)$ and $\theta(\eta)$ when $S=0.1, \varphi_{hnf}=0.02, R=1, Ec=0.1$ and $\Pr=6.2$. Therefore, reduces the skin friction and rises the heat transfer rate at the surface of the hybrid nanofluid.

Enhanced Knowledge in Sciences and Technology Vol. 4 No. 2 (2024) p. 8-15

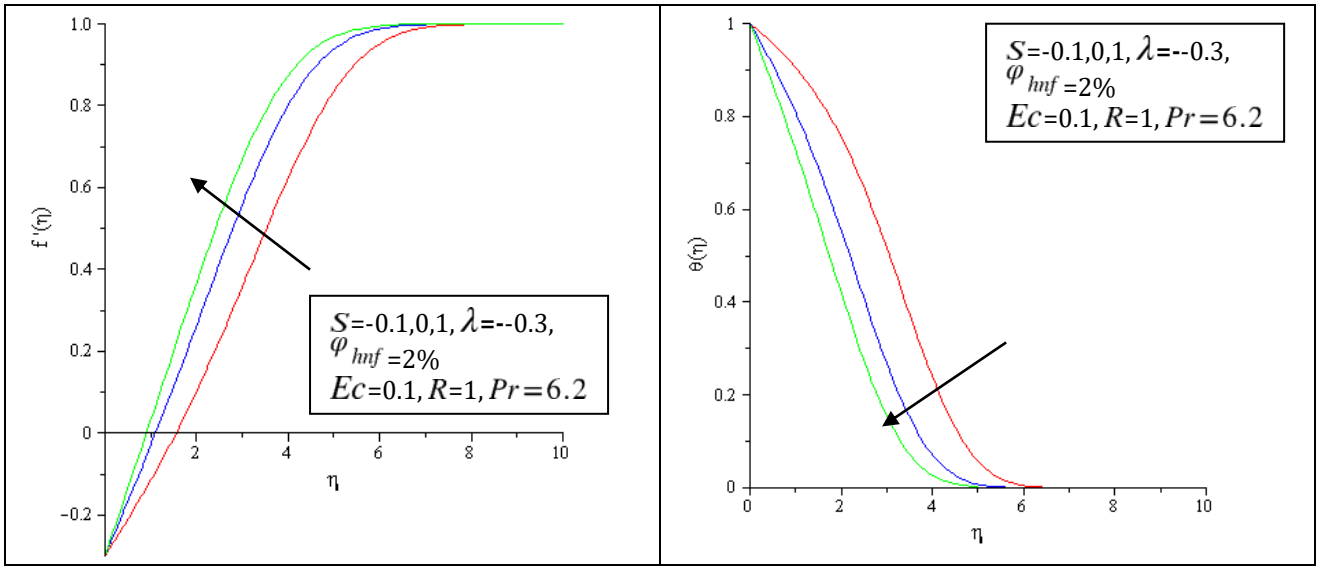

Fig. 4 Velocity profile, $f'(\eta)$ and Temperature profile, $\theta(\eta)$ for various values of S

The velocity profile $f'(\eta)$ and temperature profile $\theta(\eta)$ for various S when $\lambda = -0.3, \varphi_{hnf} = 0.02$ and $\Pr = 6.2$ are depicted in Fig. 4. It's noteworthy that the values of $f'(\eta)$ in the first solution are higher for the suction case $(S = 0.1)$. Conversely, the suction case $(S = 0.1)$ diminishes the values of $\theta(\eta)$ in the first solution.

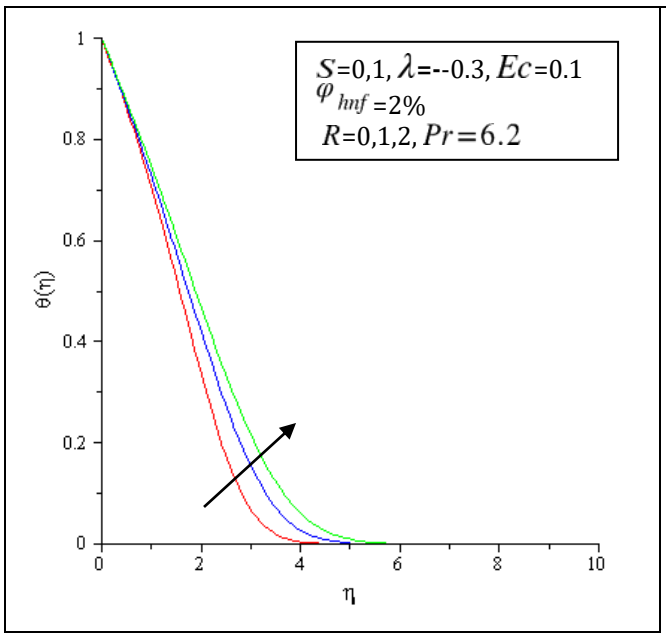

Fig. 5 Temperature profile, $\theta(\eta)$ for various of R

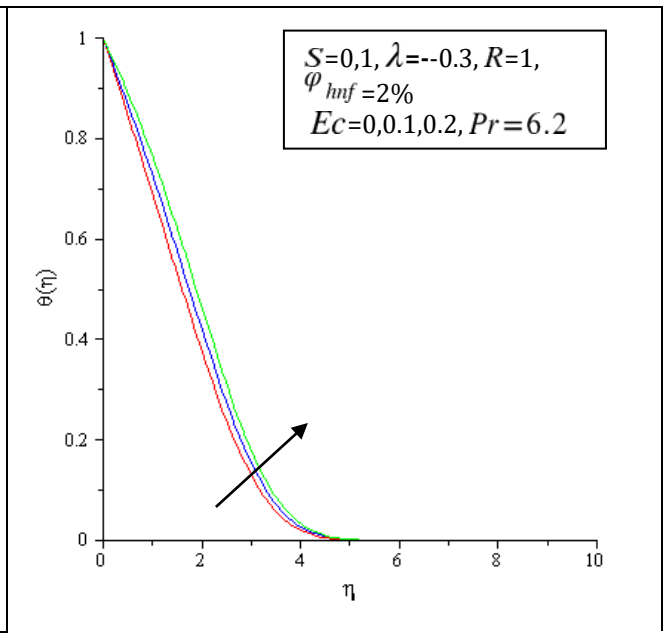

Fig. 6 Temperature profile, $\theta(\eta)$ for various values of Ec

Fig. 5 and 6 illustrate the influence of R and Ec on $\theta(\eta)$ for selected parameters. The first solution of $\theta(\eta)$ exhibits an increasing trend, while the second solution fluctuates with the rise of R. Additionally, the values of $\theta(\eta)$ for both solutions increase as Ec increases.

4. Conclusion

The present study examines the properties of Blasius flow over a permeable plate with Cu- Al_2O_3 hybrid nanoparticles, taking radiative heat transfer and viscous dissipation into consideration. The Al_2O_3 and Cu nanoparticle volume fraction, transpiration parameter, radiation parameter, Prandtl number, local Nusselt number, and Eckert number are some of these variables. Temperature and velocity characteristics are covered in the study as well. A comparison with [3] shows a high degree of consistency, validating the numerical results. An interesting discovery is that increasing the volume fraction of alumina nanoparticles produces lower temperature profiles but greater velocity profiles for a fixed amount of copper nanoparticles. The hybrid nanofluid surface experiences a decrease in the rate of heat transfer as a result of this phenomenon.

Acknowledgement

The authors would thank the Faculty of Applied Sciences and Technology, Universiti Tun Hussein Onn Malaysia for its support.

Conflict of Interest

The authors confirm that there are no conflicts of interest related to the publication of this paper.

Author Contribution

The authors confirm contribution to the paper as follows: ***study conception and design:*** *Mohammad Arief Haiqal Radzuan;* ***solve the governing equations:*** *Mohammad Arief Haiqal Radzuan;* ***analysis and interpretation of results:*** *Mohammad Arief Haiqal Radzuan, Fazlina Aman;* ***draft manuscript preparation:*** *Mohammad Arief Haiqal Radzuan, Fazlina Aman. All authors reviewed the results and approved the final version of the manuscript.*

References

[1] Olatundun, A. T., & Makinde, O. D. (2017). Analysis of Blasius flow of hybrid nanofluids over a convectively heated surface. In *Defect and Diffusion Forum* (Vol. 377, pp. 29-41). Trans Tech Publications Ltd.

[2] Waini, I.; Ishak, A.; Pop, I. Hybrid Nanofluid Flow and Heat Transfer over a Nonlinear Permeable Stretching/Shrinking Surface. Int. J. Numer. Methods Heat Fluid Flow **2019**, 29, 3110–3127.

[3] Khashi'ie, N. S., Waini, I., Ishak, A., & Pop, I. (2020). Blasius Flow over a Permeable Moving Flat Plate Containing Cu-Al2O3 Hybrid Nanoparticles with Viscous Dissipation and Radiative Heat Transfer. *Mathematics*, *10*(8), 1281.

[4] Ahmad, S., Rohni, A. M., & Pop, I. (2011). Blasius and Sakiadis problems in nanofluids. *Acta Mechanica*, *218*, 195-204.

[5] Afridi, M. I., & Qasim, M. (2019). Second law analysis of Blasius flow with nonlinear Rosseland thermal radiation in the presence of viscous dissipation. *Propulsion and Power Research*, *8*(3), 234-242.

[6] Muhammad, K., Hayat, T., & Alsaedi, A. (2021). Heat transfer analysis in slip flow of hybrid nanomaterial (Ethylene Glycol+ Ag+ CuO) via thermal radiation and Newtonian heating. *Waves in Random and Complex Media*, 1-21.

[7] Gangadhar, K.; Bhargavi, D.N.; Kannan, T.; Venkata Subba Rao, M.; Chamkha, A.J. Transverse MHD Flow of Al2O3-Cu/H2O Hybrid Nanofluid with Active Radiation: A Novel Hybrid Model. Math. Methods Appl. Sci. **2020**, 1–19.

[8] Takabi, B.; Salehi, S. Augmentation of the Heat Transfer Performance of a Sinusoidal Corrugated Enclosure by Employing Hybrid Nanofluid. Adv. Mech. Eng. **2014**, 6, 147059.